

Ultrathin $\text{Al}_{1-x}\text{Sc}_x\text{N}$ for low-voltage driven ferroelectric-based devices

Georg Schönweger, *Student Member, IEEE*, Md Redwanul Islam, *Student Member, IEEE*, Niklas Wolff, Adrian Petraru, Lorenz Kienle, Hermann Kohlstedt, Simon Fichtner, *Member, IEEE*

Abstract—Thickness scaling of ferroelectricity in $\text{Al}_{1-x}\text{Sc}_x\text{N}$ is a determining factor for its potential application in neuromorphic computing and memory devices. In this letter, we report on ultrathin (10 nm) $\text{Al}_{0.72}\text{Sc}_{0.28}\text{N}$ films that are ferroelectrically switchable at room temperature. All-epitaxial $\text{Al}_{0.72}\text{Sc}_{0.28}\text{N}/\text{Pt}$ heterostructures are grown by magnetron sputtering onto GaN/sapphire substrates followed by an *in situ* Pt capping approach to avoid oxidation of the $\text{Al}_{0.72}\text{Sc}_{0.28}\text{N}$ film surface. Structural characterization by X-ray diffraction and transmission electron microscopy reveals the established epitaxy. The thus obtained high-quality interfaces in combination with the *in situ* capping is expected to facilitate ferroelectric switching of $\text{Al}_{1-x}\text{Sc}_x\text{N}$ in the ultrathin regime. The analysis of the relative permittivity and coercive field dependence on the $\text{Al}_{0.72}\text{Sc}_{0.28}\text{N}$ film thicknesses in the range of 100 nm down to 10 nm indicates only moderate scaling effects, suggesting that the critical thickness for ferroelectricity is not yet approached. Furthermore, the deposited layer stack demonstrates the possibility of including ultrathin ferroelectric $\text{Al}_{1-x}\text{Sc}_x\text{N}$ into all-epitaxial GaN-based devices using sputter deposition techniques. Thus, our work highlights the integration and scaling potential of all-epitaxial ultrathin $\text{Al}_{1-x}\text{Sc}_x\text{N}$ offering high storage density paired with low voltage operation desired for state of the art ferroelectric memory devices.

Index Terms—aluminum-scandium-nitride ($\text{Al}_{1-x}\text{Sc}_x\text{N}$), ultrathin, ferroelectric, gallium nitride, epitaxial growth

I. INTRODUCTION

THE high coercive field (E_c) and the high, stable remanent polarization separates the ferroelectric properties recently discovered in materials with wurtzite-type structure from classical ferroelectrics [1]–[4]. This raises hopes for particularly good scalability of wurtzite-type based ferroelectric devices. In addition, the CMOS compatibility and the well established industrial deposition process make $\text{Al}_{1-x}\text{Sc}_x\text{N}$ thin films highly attractive for building novel neuromorphic computing and memory devices such as ferroelectric field-effect transistors (FeFET) and ferroelectric tunnel junctions (FTJ) [5]–[9]. Furthermore, it is expected that wurtzite-type ferroelectrics such as $\text{Al}_{1-x}\text{Sc}_x\text{N}$ introduce ferroelectricity into III-N technology, resulting in a straightforward approach to realize embedded memory. Recently, ferroelectric all-epitaxial all-wurtzite type $\text{Al}_{1-x}\text{Sc}_x\text{N}/\text{GaN}$ heterostructures were demonstrated [10], [11]. However, a very low film thickness of the ferroelectric layer is needed for following the general trend of miniaturization and increasing storage density in all of the aforementioned devices. In this context, $\text{Al}_{1-x}\text{Sc}_x\text{N}$ offers high scalability due to its high E_c , making it possible to tailor the film thickness to the ultrathin regime to achieve reasonable memory windows and low operating voltages [12]. Furthermore, in terms of

device design, ultrathin ferroelectric films are a prerequisite for building FTJs [7]. However, reducing the thickness to the ultrathin regime (< 30 nm) is often accompanied with a material-specific diminution of the remanent polarization or results in a total loss of ferroelectricity [13]. Up to now, only a small number of studies on the thickness scaling properties of ferroelectric $\text{Al}_{1-x}\text{Sc}_x\text{N}$ were conducted, revealing ferroelectricity for ≈ 20 nm film thickness at room temperature as well as for ≈ 10 nm film thickness at elevated temperatures (373 K) [14]–[16]. Here we present our recent results on 10 nm thick epitaxial $\text{Al}_{0.72}\text{Sc}_{0.28}\text{N}$ grown on epitaxial Pt/GaN templates using sputter deposition. Typical butterfly-shaped capacitance-voltage ($C - U$) loops were recorded at room temperature, demonstrating clearly distinguishable ferroelectric switching. Thus, the general feasibility of ultrathin $\text{Al}_{1-x}\text{Sc}_x\text{N}$ for future device integration and low voltage operation is demonstrated.

II. DEVICE FABRICATION AND CHARACTERIZATION METHODS

All films were grown by sputter deposition in an Oerlikon (now Evatec) MSQ 200 multisource system on top of commercially available GaN/sapphire substrates. A 12 nm thick epitaxial Pt layer (bottom electrode) was DC-sputtered at 500 °C, 600 W, and 50 sccm Kr flow. XRD measurements were performed using monochromatic K_α radiation in a Seifert XRD 3000 PTS system (θ - 2θ scan) as well as in a Rigaku SmartLab diffractometer (Phi-scan). The $\text{Al}_{0.72}\text{Sc}_{0.28}\text{N}$ thin films were grown by pulsed-DC co-sputtering at 450 °C, details about the process can be found elsewhere [17], [18]. The 10 nm thick $\text{Al}_{0.72}\text{Sc}_{0.28}\text{N}$ layer was capped *in situ* with 100 nm thick Pt. Square top-electrodes were structured via lithography and ion beam etching (IBE, Oxford Instruments Ionfab 300). Capacitance measurements were performed on a Hewlett Packard 4284A Precision LCR meter. A cross-section specimen of the *in situ* capped 10 nm thick $\text{Al}_{0.72}\text{Sc}_{0.28}\text{N}$ sample has been prepared using a standard focused ion beam (FIB) procedure and analyzed using high-resolution transmission electron microscopy (HRTEM, Tecnai F30, operated at 300 kV, field emission gun) and Fast Fourier Transform (FFT) patterns.

III. RESULTS AND DISCUSSIONS

The voltage dependence of the relative permittivity (ϵ_r) is depicted in Fig. 1. The butterfly-shaped curve (black) demonstrates distinguishable ferroelectric switching of the 10 nm thick $\text{Al}_{0.72}\text{Sc}_{0.28}\text{N}$ film. Additionally non switching half-

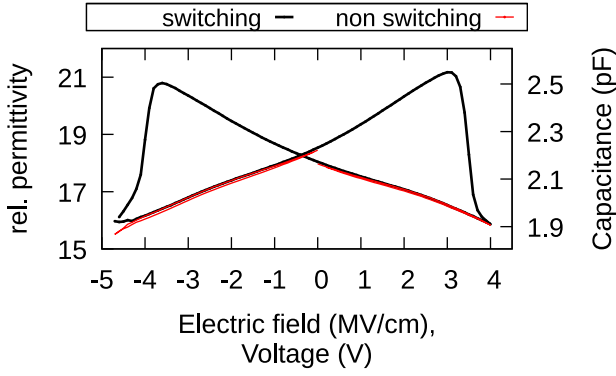


Fig. 1. Relative permittivity and capacitance as a function of the applied voltage and electric field for Pt(100 nm)/Al_{0.72}Sc_{0.28}N(10 nm)/Pt(12 nm) capacitors deposited on a GaN/sapphire template. The non switching half-loops (red) were recorded by previously switching the capacitor to the respective polarity. Measured on 10 x 10 μm^2 pads with a small signal of 1 V_{pp} at 100 kHz swept in 0.1 V steps with a delay of 300 ms per step.

loops (red) were recorded by measuring twice in the same direction. No hysteretic behaviour is observed for the non-switching half-loops, thus giving additional evidence that the butterfly-shaped hysteresis for the switching loop originates from ferroelectric switching. Previously, the coercive field in Al_{1-x}Sc_xN thin films was observed to be almost independent of film thickness down to 27 nm [14]. Similarly, the E_c fields determined via C - U loops in this study, as depicted in Fig. 2, is not changing considerably when decreasing the film thickness from 100 nm to 50 nm, while at 20 nm and especially at 10 nm film thickness, a moderate increase of the coercive field by about 20% is observed.

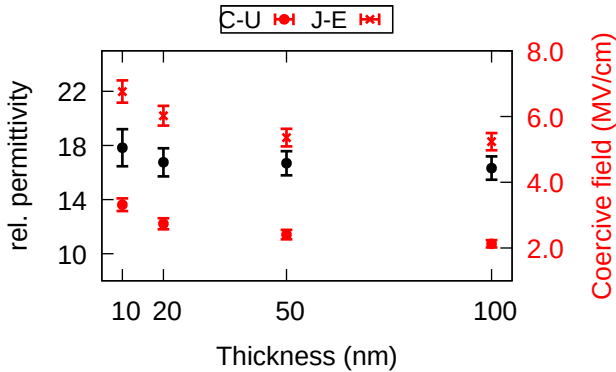


Fig. 2. ϵ_r and E_c in dependence of Al_{0.72}Sc_{0.28}N film thickness. ϵ_r was measured at 100 kHz, 100 mV at 0 V bias. E_c was determined via measuring $C-U$ loops keeping the time for a full sweep constant for the various film thicknesses as well as via $J-E$ using a sinus signal at 80 kHz. The error bars were calculated using an estimated capacitor side-length error of 0.4 μm , an estimated thickness error of 5 % and an estimated error for determination of the E_c . Additionally for E_c determination via $C-U$ loops the step width of the respective voltage sweep was included in the error calculation.

This is in strong contrast to classical ferroelectrics, e.g. the perovskites (PZT, BTO, etc.), where a pronounced increase of E_c with decreasing film thickness is observed [13], [19]. Furthermore, the often reported degradation of ferroelectric properties due to a non-switching interfacial layer (dead layer [20]) in ultrathin films is typically accompanied by a de-

crease of ϵ_r [19], [21]. Thus, ferroelectricity in 10 nm thick Al_{1-x}Sc_xN appears to be not yet influenced considerably by such interfacial effects. The non-scaling of E_c and ϵ_r with thickness leads to our conclusion that a critical thickness in Al_{1-x}Sc_xN is not yet approached at 10 nm and stable ferroelectricity can be expected also for films < 10 nm thickness.

The θ - 2θ scan depicted in Fig. 3 (left) reveals the expected out-of-plane 111 orientation for Pt and 0002 orientation for GaN. Laue oscillations, which are sensitive to crystalline disorder, are appearing for the Pt 111 reflection [22]. The thus

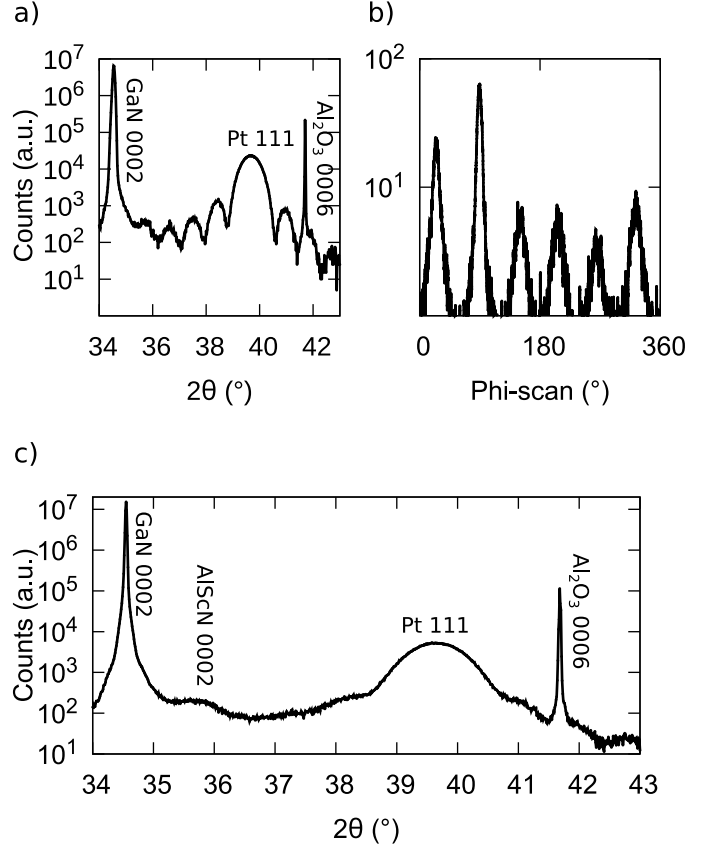


Fig. 3. a) θ - 2θ scan and b) smoothed phi-scan for the non-specular Pt 131 reflection (right) of 12 nm Pt on GaN/sapphire. c) θ - 2θ of the film shown in a) after deposition of 10 nm Al_{0.72}Sc_{0.28}N followed by 5 nm in-situ capping with Pt.

expected high crystallinity is confirmed by rocking curve (RC) measurements (not shown here) of the 111 Pt reflection; the full width at half maximum (FWHM) of 0.1 $^\circ$ is indicative of a strain and defect-poor crystalline phase with high out-of-plane orientation. Furthermore, the distinct Laue oscillations allow to determine the thickness (t) of the ordered crystal volume [22].

$$t = \frac{3\lambda}{2 \sin \theta_1 - \sin \theta_{-1}} \quad (1)$$

Using equation 1, with θ_1 and θ_{-1} corresponding to the maximum of the peaks right and left from the center Pt 111 reflection, an average film thickness of 11 nm is determined.

The in-plane ordering was resolved by recording a phi-scan of the non-specular 131 Pt reflection, depicted in Fig. 3 (right).

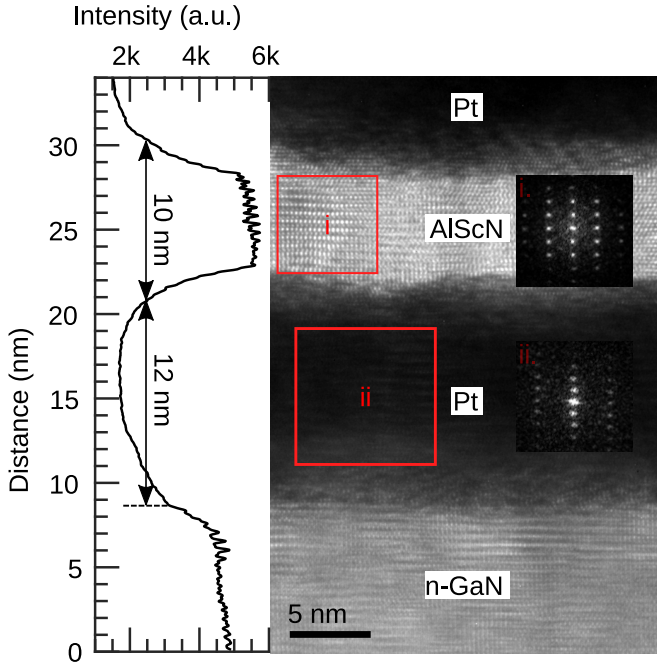


Fig. 4. HRTEM image (right) and corresponding averaged thickness profile (left) of the Pt(100 nm)/Al_{0.72}Sc_{0.28}N(10 nm)/Pt(12 nm)/GaN/sapphire heterostructure. In the inset, the FFT pattern for Al_{0.72}Sc_{0.28}N (i) and Pt (ii) is depicted.

A 6-fold symmetry is visible, evidencing epitaxial (in-plane ordered) growth.

The intensity profile across the HRTEM micrograph is shown in Fig. 4 and film thicknesses of 10 nm for Al_{0.72}Sc_{0.28}N and 12 nm for Pt are determined on local average. The latter is in excellent agreement with the Pt thickness calculated using equation 1. The FFT pattern clearly reveals an epitaxial growth for both layers. The epitaxial growth in combination with the *in situ* capping of Al_{1-x}Sc_xN to avoid oxidation is expected to have a significant impact on the ferroelectric switching behaviour, especially for ultrathin films. The blurred interfaces present in the HRTEM image are attributed to the finite roughness of the heterostructure.

IV. CONCLUSION

Distinguishable ferroelectric switching of 10 nm thick Al_{0.72}Sc_{0.28}N was demonstrated at room temperature. Largely constant coercive fields and constant ϵ_r for films ranging from 100 nm down to 10 nm thickness were confirmed. Thus, no indications of instabilities of the ferroelectric phase or considerable contributions from dead layers are present. Therefore, it is expected that further potential remains to scale ferroelectric Al_{1-x}Sc_xN to even lower thicknesses. These results highlight the general feasibility of using Al_{1-x}Sc_xN as an active layer for integrated electronic devices with low operating voltage and high storage density.

ACKNOWLEDGMENT

This work was supported by the project “ForMikro-SALSA” (grant no. 16ES1053) from the Federal Ministry of Education and Research (BMBF) and the Deutsche Forschungsgemeinschaft (DFG) under the scheme of the collaborative research centers (CRC) 1261 and 1461.

REFERENCES

- [1] S. Fichtner, N. Wolff, F. Lofink, L. Kienle, and B. Wagner, “AlScN: A III-V semiconductor based ferroelectric,” *Journal of Applied Physics*, vol. 125, no. 11, p. 114103, mar 2019.
- [2] K. Ferri, S. Bachu, W. Zhu, M. Imperatore, J. Hayden, N. Alem, N. Giebink, S. Trolier-McKinstry, and J.-P. Maria, “Ferroelectrics everywhere: Ferroelectricity in magnesium substituted zinc oxide thin films,” *Journal of Applied Physics*, vol. 130, no. 4, p. 044101, jul 2021.
- [3] J. Hayden, M. D. Hossain, Y. Xiong, K. Ferri, W. Zhu, M. V. Imperatore, N. Giebink, S. Trolier-McKinstry, I. Dabo, and J.-P. Maria, “Ferroelectricity in boron-substituted aluminum nitride thin films,” *Physical Review Materials*, vol. 5, no. 4, p. 044412, apr 2021.
- [4] D. Wang, P. Wang, B. Wang, and Z. Mi, “Fully epitaxial ferroelectric ScGaIn grown on GaN by molecular beam epitaxy,” *Applied Physics Letters*, vol. 119, no. 11, p. 111902, sep 2021.
- [5] H. Mulaosmanovic, T. Mikolajick, and S. Slesazeck, “FeFETs for neuromorphic systems,” in *Topics in Applied Physics*. Springer Singapore, 2020, pp. 399–411.
- [6] T. Schenk, M. Pešić, S. Slesazeck, U. Schroeder, and T. Mikolajick, “Memory technology—a primer for material scientists,” *Reports on Progress in Physics*, vol. 83, no. 8, p. 086501, jul 2020.
- [7] E. Y. Tsymlal and H. Kohlstedt, “Tunneling across a ferroelectric,” *Science*, vol. 313, no. 5784, pp. 181–183, jul 2006.
- [8] H. Kohlstedt, N. A. Pertsev, J. R. Contreras, and R. Waser, “Theoretical current-voltage characteristics of ferroelectric tunnel junctions,” *Physical Review B*, vol. 72, no. 12, p. 125341, sep 2005.
- [9] X. Liu, D. Wang, J. Zheng, P. Musavigharavi, J. Miao, E. A. Stach, R. H. O. III, and D. Jariwala, “Post-cmos compatible aluminum scandium nitride/2d channel ferroelectric field-effect-transistor,” 2020.
- [10] P. Wang, D. Wang, N. M. Vu, T. Chiang, J. T. Heron, and Z. Mi, “Fully epitaxial ferroelectric ScAlN grown by molecular beam epitaxy,” *Applied Physics Letters*, vol. 118, no. 22, p. 223504, may 2021.
- [11] G. Schönweger, A. Petraru, M. R. Islam, N. Wolff, B. Haas, A. Hammud, C. Koch, L. Kienle, H. Kohlstedt, and S. Fichtner, “From fully strained to relaxed: Epitaxial ferroelectric Al_{1-x}Sc_xN for III-n technology,” *Advanced Functional Materials*, p. 2109632, feb 2022.
- [12] H. Mulaosmanovic, E. T. Breyer, T. Mikolajick, and S. Slesazeck, “Ferroelectric FETs with 20-nm-thick HfO₂ layer for large memory window and high performance,” *IEEE Transactions on Electron Devices*, vol. 66, no. 9, pp. 3828–3833, sep 2019.
- [13] H. Qiao, C. Wang, W. S. Choi, M. H. Park, and Y. Kim, “Ultra-thin ferroelectrics,” *Materials Science and Engineering: R: Reports*, vol. 145, p. 100622, jul 2021.
- [14] S. Fichtner, G. Schönweger, T.-N. Kreutzer, A. Petraru, H. Kohlstedt, F. Lofink, and B. Wagner, “Ferroelectricity in alscn: Switching, imprint and sub-150 nm films,” in *Proc. 2020 IEEE ISAF*, 2020.

- [15] D. Wang, J. Zheng, P. Musavigharavi, W. Zhu, A. C. Foucher, S. E. Troler-McKinstry, E. A. Stach, and R. H. Olsson, "Ferroelectric switching in sub-20 nm aluminum scandium nitride thin films," *IEEE Electron Device Letters*, vol. 41, no. 12, pp. 1774–1777, dec 2020.
- [16] R. Mizutani, S. Yasuoka, T. Shiraishi, T. Shimizu, M. Uehara, H. Yamada, M. Akiyama, O. Sakata, and H. Funakubo, "Thickness scaling of $\text{Al}_{0.8}\text{Sc}_{0.2}\text{N}$ films with remanent polarization beyond $100 \mu\text{C cm}^{-2}$ around 10 nm in thickness," *Applied Physics Express*, vol. 14, no. 10, p. 105501, sep 2021.
- [17] S. Fichtner, T. Reimer, S. Chemnitz, F. Lofink, and B. Wagner, "Stress controlled pulsed direct current co-sputtered $\text{Al}_{1-x}\text{Sc}_x\text{N}$ as piezoelectric phase for micromechanical sensor applications," *APL Materials*, vol. 3, no. 11, p. 116102, nov 2015.
- [18] S. Fichtner, N. Wolff, G. Krishnamurthy, A. Petraru, S. Bohse, F. Lofink, S. Chemnitz, H. Kohlstedt, L. Kienle, and B. Wagner, "Identifying and overcoming the interface originating c-axis instability in highly sc enhanced AlN for piezoelectric micro-electromechanical systems," *Journal of Applied Physics*, vol. 122, no. 3, p. 035301, jul 2017.
- [19] N. A. Pertsev, J. R. Contreras, V. G. Kukhar, B. Hermanns, H. Kohlstedt, and R. Waser, "Coercive field of ultrathin $\text{Pb}(\text{Zr}_{0.52}\text{Ti}_{0.48})\text{O}_3$ epitaxial films," *Applied Physics Letters*, vol. 83, no. 16, pp. 3356–3358, oct 2003.
- [20] C. Zhou and D. M. Newns, "Intrinsic dead layer effect and the performance of ferroelectric thin film capacitors," *Journal of Applied Physics*, vol. 82, no. 6, pp. 3081–3088, sep 1997.
- [21] M. Stengel and N. A. Spaldin, "Origin of the dielectric dead layer in nanoscale capacitors," *Nature*, vol. 443, no. 7112, pp. 679–682, oct 2006.
- [22] X. Castel, M. Guilloux-Viry, A. Perrin, J. Lesueur, and F. Lallu, "High crystalline quality CeO_2 buffer layers epitaxied on sapphire for $\text{YBa}_2\text{Cu}_3\text{O}_7$ thin films," *Journal of Crystal Growth*, vol. 187, no. 2, pp. 211–220, may 1998.